A Finite-Difference based Method for the Design of Gradient Coils in MRI

L. Xia[1], M. Zhu[1], G. Shou[1], F. Liu[2], and S. Crozier[2]
[1]Department of Biomedical Engineering, Zhejiang University, Hangzhou, China, People's Republic of, [2]School of Information Technology & Electrical Engineering, University of Queensland, Brisbane, Australia

Introduction There exist a number of numerical techniques for the design of gradient coils in MRI. In this work, a finite difference (FD) method based scheme is proposed for MRI coil designs. Given that the FD method in time-domain (FDTD) is the method of choice to model MRI field/tissue interactions in RF and in gradient applications [1], having a unified framework of FD allows a complete electromagnetic (EM) model for the design and analysis of an MRI system, which includes all field generating units and an electrical model of a patient. For example, the eddy currents generated in the cryostat and RF structure (volume resonator, array, shielding) due to gradient switching can be evaluated while patient's SAR levels are calculated. These lead to a better understanding of the fields within patients and general temporal field behaviour during an MRI scan, thus offering insight into fundamental EM problems related to MRI and possibly leading to new discoveries. In addition, the proposed FD algorithm is mathematically straightforward but versatile; it simply approximates the continuous current density over a 2D or 3D surface using a finite-difference formulation which is much easier than other schemes such as the Finite-Element Method (FEM) or Boundary Element Method (BEM) (2). This abstract describes the algorithm and provides two shielded gradient coil design examples: planar and cylindrical X-gradient coils.

X-gradient coil designs *Governing equations* By way of example, we consider the X-gradient coil configurations illustrated in Fig.1. In the coil space, with the current density $\vec{J}(\vec{r}') = J_r\vec{e}_r + J_\theta\vec{e}_\theta + J_z\vec{e}_z$ (Eq.(1)) at the source point $\vec{r}'(r,\theta,z)$, we can obtain the expression of the z-component of magnetic flux density at the field point (x_f,y_f,z_f) as $B_z(x_f,y_f,z_f) = \frac{\mu_0}{4\pi}\int_{V'}(J_r S - J_\theta Q)/T\, rdrd\theta dz$ (Eq.(2)). For the biplanar gradient coils design case, the primary layer is locate at $z_0=\pm a$ and the shielding layer is locate at $z_0=\pm b$,thus the current density can be expressed as the following equation $\vec{J} = (J_r^{(\pm a)} + J_r^{(\pm b)})\vec{e}_r + (J_\theta^{(\pm a)} + J_\theta^{(\pm b)})\vec{e}_\theta$ (Eq.(3)). Then based on Eq.2, we have the equation $B_z(x_f,y_f,z_f) = \frac{\mu_0}{4\pi}\int_0^{2\pi}\int_0^{R_a}\left(J_r^{(\pm a)}S - J_\theta^{(\pm a)}Q\right)/T^{(\pm a)}\, rdrd\theta + \frac{\mu_0}{4\pi}\int_0^{2\pi}\int_0^{R_b} J_r^{(\pm b)}S - J_\theta^{(\pm b)}Q/T^{(\pm b)}\, rdrd\theta$ (Eq.(4)). For the cylindrical gradient coils design case, the primary layer is located at the cylinder with a radius of R_a and the shielding layer is locate at the cylinder with a radius R_b, thus the corresponding current density can be expressed as $\vec{J} = (J_\theta^{(a)} + J_\theta^{(b)})\vec{e}_\theta + (J_z^{(a)} + J_z^{(b)})\vec{e}_z$ (Eq.(5)). Hence we can have the field equation as $B_z(x_f,y_f,z_f) = \frac{\mu_0}{4\pi}\int_0^{2\pi}\int_{-L_a}^{L_a} -J_\theta^{(a)}Q/T^{(a)}\, R_a d\theta dz + \frac{\mu_0}{4\pi}\int_0^{2\pi}\int_{-L_b}^{L_b} -J_\theta^{(b)}Q/T^{(b)}\, R_b d\theta dz$ (Eq.(5)). In the above equations, T,S,Q are the intermediate terms and the corresponding expression is $S = -x_f\sin\theta + y_f\cos\theta, Q = x_f\cos\theta + y_f\sin\theta - r, T = \left(S^2 + Q^2 + (z - z_f)^2\right)^{1.5}$ (Eq.(6)), in which the superscripts (a) or (b) means the primary coils or shielding coils. If the current densities are expressed with scalar potentials, $J_r = \partial\Psi/(r\partial\theta), J_\theta = -\partial\Psi/\partial r$ for the biplanar coil and $J_\theta = \partial\Psi/\partial z, J_z = -\partial\Psi/(r\partial\theta)$ for the cylindrical coil, then we can find the gradient coil pattern using the well-known stream function scheme (3).

Discretization of the coil space using the finite difference method As shown in Fig.1, the coil space can be discretized into desired mesh structures and approximated using central difference formula. Then taking an example of biplanar, primary, X-gradient coil, the B_z field can be expressed as

$$B_z(x_f,y_f,z_f) = \frac{\mu_0}{4\pi}\sum_i\sum_j\left[\left(\Psi^{\pm a}(i,j+1) - \Psi^{\pm a}(i,j)\right)S\Delta r + \left(\Psi^{\pm a}(i+1,j) - \Psi^{\pm a}(i,j)\right)Qr\Delta\theta\right]/T^a \text{ (Eq.(7))}$$

Solving the inverse problem using a regularization scheme After setting the field points over the DSV, a linear equation can be constructed and then solved for the coil patterns. As shown in Fig.1, the DSV region was sampled with a number of field points p_k over the DSV surface. The B_z field at the field point p_k can be expressed as $B_z(p_k) = \sum_{i=1}^{G}\sum_{j=1}^{H} A_{ij}\Psi(i,j)$ (Eq.(8)) where G, H: total number of nodes in the two directions in the investigated coil surface; $B_z(p_k)$ is the target magnetic flux density at the field point p_k ; $\Psi(i,j)$ denotes the scalar potential or stream function at the source node (i,j) ; $A_{i,j}$ is the sensitivity coefficient. With a total control number of U and total source nodes of V, we can obtain the following linear system equations $A\Psi = B$ (Eq.(9)), which is a typical inverse problem to solve. As the system matrix is ill-posed, we used the Tikhonov regularization to find an approximated solution for Eq.(9). To reduce some possible local hot spots in the designed coil surface, a penalty function $F = \int_0^R\int_0^{2\pi}\left(\left(\partial J_r/(r\partial\theta)\right)^2 + \left(\partial(rJ_\theta)/(r\partial r)\right)^2\right)rd\theta dr$ (Eq.(10)) has been used to penalize the inverse solution procedure for the planar coil and for the cylindrical coil, the penalty function is $F = \int_{-L/2}^{L/2}\int_0^{2\pi}\left(\left(\partial J_z/(r\partial\theta)\right)^2 + \left(\partial J_\theta/\partial z\right)^2\right)rd\theta dz$ (Eq.(11)). Fig.2 is the designed gradient coil pattern. For these designs, the regularization parameter used was 7.78e-10 for the biplanar coils and 4e-10for the cylindrical coils. Fig.3 shows the gradient field profiles, it can be seen that the designs offer excellent gradient linearity (<5%) over the DSV. More importantly, the wires are well distributed and local hot spots have been reduced.

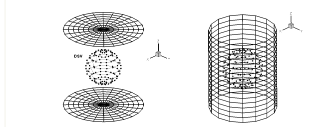

Fig.1 The discretizations of the X-gradient coil space using finite-difference mesh structures and the field sampling over the DSV. For the biplanar gradient coils(Left), the plates are uniformly meshed in both radial and azimuthal directions; and the space for the cylindrical gradient coils(Right) have been uniformly meshed in both azimuthal and longitudinal directions.

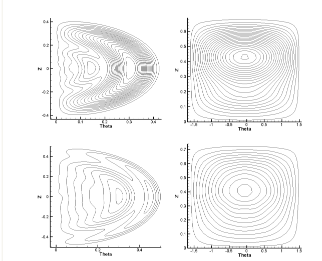

Fig.2 The designed biplanar X-gradient coil. Left: biplanar primary coil (upper) and shielding coil (lower),the radii of the circular plates are R_a=0.43m, R_b=0.5m and a=0.25m,b=0.35m. Right: cylindrical primary coil (upper) and shielding coil(lower), the radii of the cylinders are R_a=0.32m, R_b=0.39m, and the length of the cylinder are L_a=1.38m, L_b=1.48m .

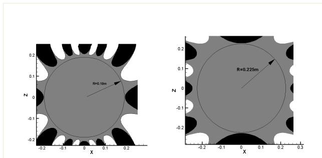

Fig.3 The gradient field profile over the DSV. The DSV sizes/target gradient strength: 0.38m/6.25mT/m (bilplanar coils) and 0.225m/25mT/m (cylindrical coils) .

Discussion and conclusion We have shown that the FD based approach is very easy to implement for conventional gradient coil designs incorporating engineering constraints. The developed method can also be used for unconventional designs with corresponding FD mesh structures. We will include this gradient design scheme into our finite-difference based EM platform allowing an integrated design framework based around the FD method including gradients, RF and patient interactions.

Reference

[1] F. Liu and S. Crozier, *Phys Med Biol*, 39: 1835-1851 (2004). [2] G. Shou, L. Xia, F. Liu, M. Zhu and S. Crozier, *IEEE Trans. Magn.*, 46: 1052-1059 (2010). [3] M.A. Brideson, L.K. Forbes, and S.Crozier, *Concepts Magn Reson*, 14: 9-18 (2002).